ACOUSTIC BUBBLE SIZING USING TWO FREQUENCY EXCITATION TECHNIQUES

A D Phelps and T G Leighton

Institute of Sound and Vibration Research, University of Southampton, Southampton SO9 5NH

1. ABSTRACT

Studies into a range of oceanic effects (atmosphere/ocean gas flux, near surface acoustic propagation, etc.) often require knowledge of the size, number and distribution of bubbles, information which is also required in certain industrial or clinical systems. Because bubbles are excellent scatterers of sound, with well-defined acoustic resonances which (to a first approximation) are inversely proportional to their size, these measurements lend themselves towards the use of acoustics. The nonlinearity inherent in high-amplitude bubble pulsations may be used to detect resonance, and this can be exploited using two sound fields projected at the bubble: one high fixed imaging frequency and another lower pump frequency. When the latter is resonant with the bubble, the nonlinearity gives rise to sum-and-difference coupling of the imaging frequency with the bubble resonance, and with harmonics, subharmonics and ultraharmonics of this resonance. From these the bubble radius can be determined. This paper gives details of investigations into the suitability of this method to actively size bubbles of unknown radius and distribution, and discusses its accuracy and limitations. In addition, the feasibility of automated high-resolution bubble sizing is examined using specialised signal processing and heterodyning techniques.

2. INTRODUCTION

Recent work investigating the transport of gases from the atmosphere into the oceans has identified the action of bubbles as contributing an important nonlinearity into this flux[1,2]. A knowledge of the size and number of bubbles in a fluid media has also been used in studies into decompression sickness[3], contrast echocardiography[4] and monitoring the coolant in nuclear reactors[5]. Acoustic scattering from bubbles at resonance (the frequency of which varies approximately inversely with the bubble radius[6]) is several orders greater than off resonance[7]. Common detection techniques which use this acoustic scattering (linear resonant backscatter[8], Doppler methods[9] and second harmonic generation[10]) are all limited[7,11]. The method outlined in this paper utilises the nonlinear coupling of two sound fields which occurs in bubbles at resonance. The bubble is insonated with two frequencies, one a high fixed frequency ω_i (called the *imaging* frequency), and another lower frequency ω_p (called the *pump* frequency). When the pump frequency is at or close to the bubble resonance, the nonlinear pulsations of the bubble will couple the two sound fields together, so that the signal returned from the bubble consists of the amplitude modulated imaging frequency. At

resonance, the high frequencies contain, in addition to ω_i, components at $\omega_i \pm \omega_p$, $\omega_i \pm \omega_p/2$, $\omega_i \pm 3\omega_p/2$ and others at different thresholds of pumping amplitudes. Though some workers[11,12] have taken the appearance of the signal at $\omega_i \pm \omega_p$ to indicate the presence of a bubble resonant at ω_p, this is not conclusive evidence[15]. The sizing signal used in this study, $\omega_i \pm \omega_p/2$, is a less ambiguous indicator[13-15]. Both of these two coupled signals are presented in ***figure 1***.

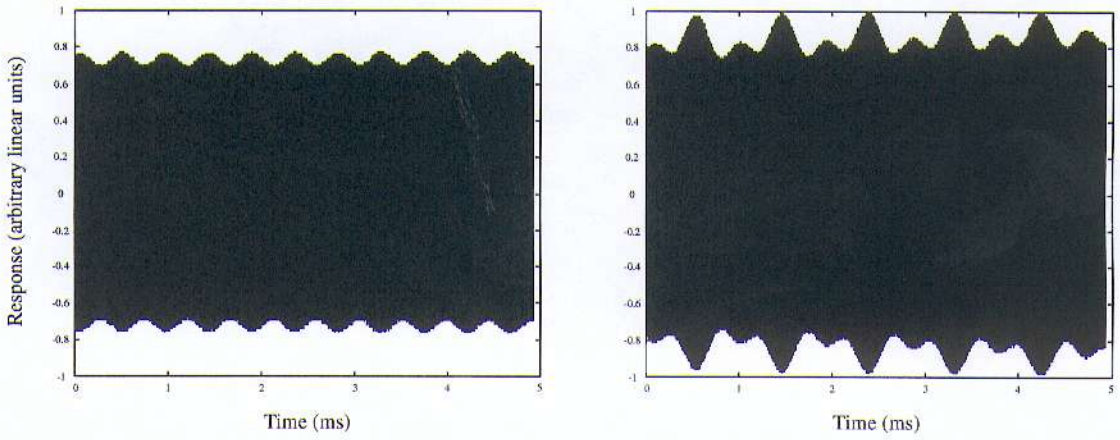

Figure 1 Returned signals sampled at 10 MHz on a LeCroy 9314L digital oscilloscope from a bubble insonated at two frequencies - the imaging signal was set at 1.1 MHz, and the bubble resonance/pump frequency at 2160 Hz. Plot (a) shows the $\omega_i \pm \omega_p$ coupling by a bubble excited at 25 Pa 0-Pk; plot (b) contains, in addition, a $\omega_i \pm \omega_p/2$ component from a bubble driven at 40 Pa 0-Pk.

The tests reported in this text were all performed on single bubbles in order to ensure that the system is not prone to erroneous triggering inherent in other signals, and to establish the methodology and protocol necessary for using the technique to size multiple bubble populations. The benefit of using the $\omega_i \pm \omega_p/2$ and considerations for the practical construction of an automated bubble sizer are discussed.

3. EXPERIMENTAL DETAILS

The tests are performed in a 1.8 m x 1.2 m x 1.2 m deep glass reinforced plastic tank which is filled with water to 1 m depth, and the experimental set-up is shown in ***figure 2***.

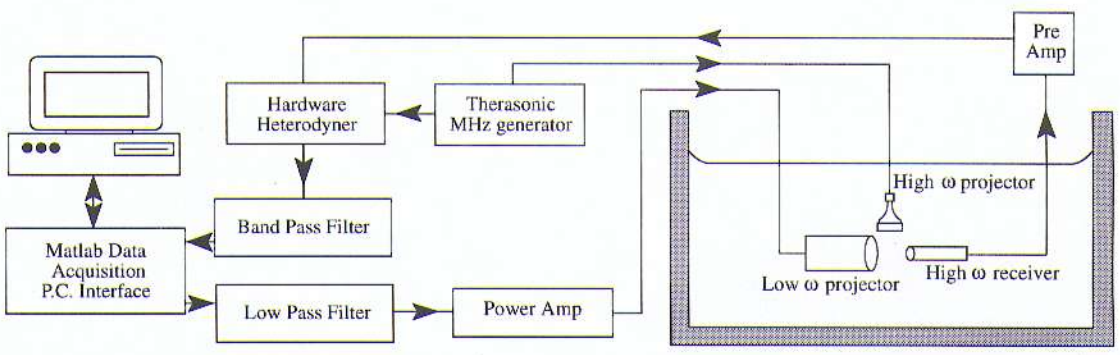

Figure 2. The equipment and experimental arrangement used in the tests. The three transducers are drawn out of the horizontal for clarity.

A Therasonic 1030 Ultrasound Generator (Electro-Medical Supplies) provides a continuous wave imaging signal at $\omega_i \approx 1.1$ MHz. The three transducers are clamped onto a rigid stainless steel cage to maintain their relative alignment from one test to the next, and the hardware and mounting was designed to minimise spurious signal coupling, as described elsewhere[15]. Both projection and detection systems were checked to ensure they introduced no harmonic distortion at the frequency locations of interest.

Signal generation and detection is controlled by a specialist MATLAB data acquisition P.C. interface package and software. This outputs the specified pumping frequencies, and simultaneously takes in data from the receiver. The MATLAB output signal is passed through a DAC, and then through a low pass reconstruction filter to remove any unwanted harmonics. This signal is amplified (Bruel and Kjaer 2713 A) and broadcast into the tank by a Gearing and Watson UW60 underwater loudspeaker. The returned signal from the bubble is picked up by an unfocused high frequency receiver (Panametrics V302 resonant at 1 MHz) and passed through a preamplifier (Panametrics 5670). This signal is then heterodyned with a dummy signal from the Therasonic, so that the imaging frequency is converted to D.C., and the signal contained above the imagining frequency reproduced at just above D.C. This allows the use of a much smaller sample rate and minimises the amount of data storage, which slowed previous measurement methods[15]. This heterodyned signal is passed through a band pass filter to prevent aliasing and remove low frequency signal components caused by water perturbations etc., and is then sampled by the MATLAB acquisition box. The time history is stored in memory, and the next pumping frequency is outputted. At the end of the data collection the time histories are FFTed for analysis. The strength of the outputted signal is amplitude corrected to invert the tank frequency response to allow a constant insonation level, and a delay of 500 cycles between the start of the bubble insonation and the data collection is introduced to allow time for any transients to decay away. The whole process of output/delay/input/storing takes around 0.4 of a second per pump frequency, of which the majority of the time is taken up with the delay phase.

4. RESULTS

The results from a single run are given in ***figure 3***. The plot shows the heterodyned output from the high frequency receiver between 0 and 3400 Hz for a single bubble insonated between 1700 Hz and 2700 Hz in discrete 25 Hz steps. The amplitude of the excitation is 54 Pa, and the bubble is tethered to a wire at a depth of 15 cm. The plot shows a ridge which is present over the entire 41 different pumping tones, and which rises up to a maximum and then decays away again. This is the signal at $\omega_i \pm \omega_p$, the maximum corresponding to the location of the bubble resonance. Behind this ridge is another much narrower signal which again has a peak at the same pump frequency location. This is the signal at $\omega_i \pm \omega_p/2$, and obviously more clearly resolves the single-bubble resonance. It is thus less likely than the $\omega_i \pm \omega_p$ signal to erroneously interpret off-resonant signal contributions as being indicators of the presence of other bubbles. The plot shows an unbroken ridge at just above 0 Hz - this is caused by side lobes around the imaging signal because the Therasonic does not generate a perfect sine wave.

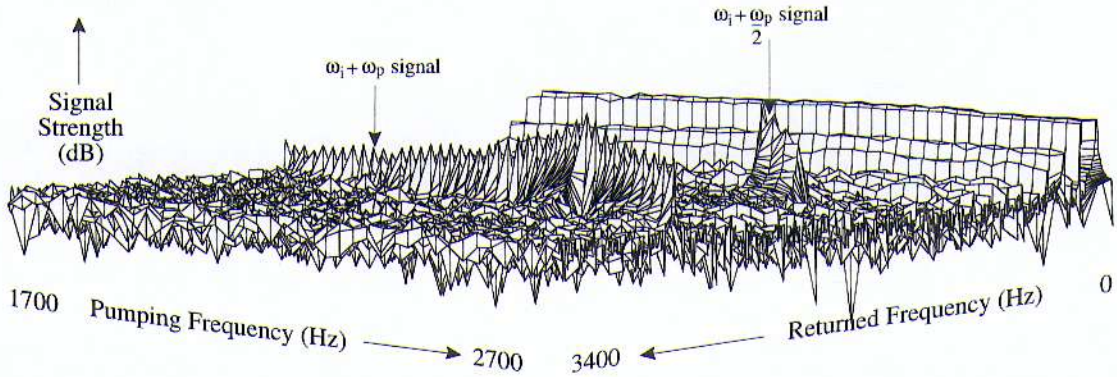

Figure 3 Mesh plot of returned signal strength through a bubble's resonance. The bubble was insonated at 54 Pa and the pumping frequency was stepped in 25 Hz intervals.

A series of tests were performed to investigate the emergence of the $\omega_i \pm \omega_p/2$ signal for different amplitudes of excitation, and the results are given in ***figure 4*** as a graph of the subharmonic height vs pumping frequency, where for each input signal the height of the power spectrum at the speculative location of its subharmonic is measured

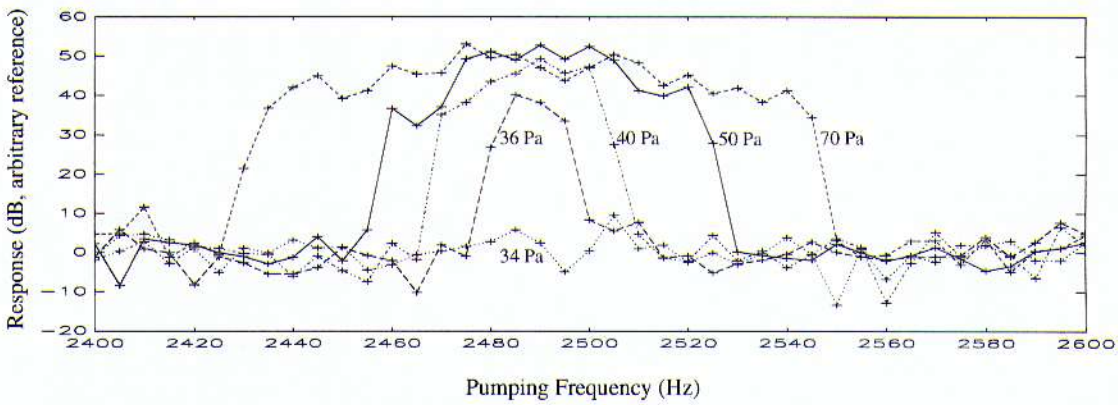

Figure 4 The variation in $\omega_i \pm \omega_p/2$ signal power from a single bubble as a function of the amplitude of the pumping signal at pressures of 34 Pa, 36 Pa, 40 Pa, 50 Pa and 70 Pa. The frequency step size is 5 Hz, and the bubble was tethered at 15 cm depth.

The bubble was insonated in 5 Hz steps from 2400 to 2600 Hz. The run was repeated with increasing pumping frequency amplitude levels, of which five are shown. When the bubble is insonated at 34 Pa no $\omega_i \pm \omega_p/2$ signal exists, but for a marginal increase in pumping amplitude to 36 Pa a strong signal emerges from the noise indicating a bubble resonance of 2485 ± 5 Hz. The span of pump frequencies over which the $\omega_i \pm \omega_p/2$ signal can be exacted increases with increasing pump amplitude, thereby decreasing the resolution of the resonance. The y axis from this plot shows the signal strength in dB with a common but arbitrary reference value: only relative comparisons are important since the signal level picked up from the heterodyner is directly proportional to the level output from the imaging projector.

The final set of tests presented demonstrate how the subharmonic threshold varies for different bubble sizes, shown in ***figure 5***. The increasing amplitude method described above was employed for a number of different bubbles resonant between 2000 and 3200 kHz, and their sum-and-difference subharmonic excitation thresholds measured. The graph also shows the least-squares fit straight line to this data, which steadily increases as the resonant frequency gets larger (and the bubbles get smaller).

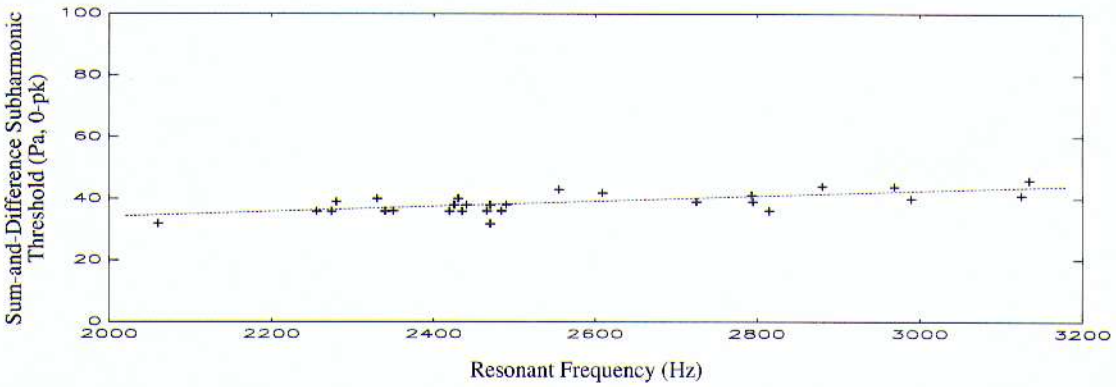

Figure 5 Plot showing the thresholds for sum-and-difference subharmonic excitation for various bubble sizes at 15 cm depth. The graph also shows the line of regression to the data.

5. DISCUSSION

It is evident from ***figure 3*** that, whilst both the $\omega_i \pm \omega_p$ and the $\omega_i \pm \omega_p/2$ signals peak at the bubble resonance, the subharmonic gives better resolution. Previous tests using this technique[11] have taken the appearance of a signal at $\omega_i \pm \omega_p$ to be an unambiguous indicator of the presence of a bubble resonant at ω_p, although the off-resonance response shows that this is clearly not so. In addition, contributions to the $\omega_i \pm \omega_p$ signal can arise from effects other than the bubble response, including turbulence and the direct action of the low frequency projector on the receiver transducer[15]. The subharmonic, however, is created by the bubble's nonlinear response to the incident pumping signal, which in turn couples with the imaging sound field, and hence is an unambiguous indicator of a bubble's presence.

The use of this method for automated bubble sizing and counting presents some interesting questions. It is clear ***(figure 4)*** that a very definite amplitude threshold exists below which no signal at $\omega_i \pm \omega_p/2$ is detected. Above this threshold a sum-and-difference subharmonic response can be exacted from a bubble when the pumping frequency is increasingly off-resonance. Thus a compromise is required between the amplitude of excitation, and the step size which the pumping signal increases by each time the data is collected. As the step size is decreased and the frequency resolution of the scan improves, the insonation amplitude must also be reduced to preserve the definition of the peak. By slightly 'under sampling' the bubble population a trade-off can exist where one bubble will give rise to a single, or at least unambiguous, subharmonic peak while the amplitude of the input signal can be set slightly higher than the threshold value for that bubble size, and hence be certain that a strong subharmonic signal will be returned. The threshold comparison results presented in ***figure 5*** show that the subharmonic emission levels vary with bubble size, but can be quantified.

6. CONCLUSIONS

When a liquid is insonated by two sound fields, the nonlinear mixing of the signals presents a way of accurately detecting and sizing gas bubbles. Exploiting the $\omega_i \pm \omega_p/2$ signal gives better size resolution and less chance of false triggering than the $\omega_i \pm \omega_p$ signal. This subharmonic signal only exists above a well defined insonation amplitude level threshold, but for only small increases in amplitude above this threshold the range of pumping frequencies over which a signal can be exacted increases rapidly. Therefore the design of an automated bubble sizer would have to ensure that the low frequency insonation level was carefully matched to this threshold, and to balance this with consideration of the frequency interval between consecutive pumping tones.

7. ACKNOWLEDGEMENTS

The authors wish to thank the Natural Environment Research Council who have funded the project, reference SIDAL 00670.

8. REFERENCES

1. **Woolf, D.K. and Thorpe, S.A.** Bubbles and the air-sea exchange of gases in near saturation conditions *Journal of Marine Research* (1991) **49** 435-466
2. **Woolf, D.K.** Bubbles and the air-sea transfer velocity of gases *Atmosphere-Ocean* (1993) **31** 451-474
3. **Belcher, E.O.** Quantification of bubbles formed in animals and man during decompression *IEEE Trans Biomed Eng* (1980) **27** 330-338
4. **Tickner, E.G.** Precision microbubbles for right side intercardiac pressure and flow measurements, in: *Contrast Echocardiography* (Eds. Meltzer, R.S. and Roeland, J.) Nijhoff, London, UK (1982)
5. **Watkins, R.D., Barrett, L.M. and McKnight, J.A.** Ultrasonic waveguide for use in the sodium coolant of fast reactors *Nucl Energy* (1988) **27** 85-89
6. **Minneart, M.** On musical air-bubbles and sounds of running water *Phil Mag* (1933) **16** 235-248
7. **Leighton, T.G.** The Acoustic Bubble (1994) *Publ: Academic Press*
8. **Fairbank, W.M. and Scully, M.O.** A new non-invasive technique for cardiac pressure measurement: resonant scattering of ultrasound from bubbles *IEEE Trans Biomed Eng* (1977) **24** 107-110
9. **Nishi, R.Y.** Ultrasonic detection of bubbles with Doppler flow transducers *Ultrasonics* (1972) **10** 173-179
10. **Miller, D.L.** Ultrasonic detection of resonant cavitation bubbles in a flow tube by their second-harmonic emissions *Ultrasonics* (1981) **19** 217-224
11. **Shankar, P.M., Chapelon, J.Y. and Newhouse, V.L.** Fluid pressure measurement using bubbles insonified by two frequencies *Ultrasonics* (1986) **24** 333-336
12. **Newhouse, V.L. and Shankar, P.M.** Bubble size measurement using the nonlinear mixing of two frequencies *JASA* (1984) **75** 1473-1477
13. **Leighton, T.G., Lingard, R.J., Walton, A.J. and Field, J.E.** Acoustic bubble sizing by combination of subharmonic emissions with imaging frequency *Ultrasonics* (1991) **29** 319-323
14. **Hardwick, A.J., Leighton, T.G., Walton, A.J. and Field, J.E.** Acoustic bubble sizing through nonlinear combinations involving parametric excitations *European Conf on Underwater Acoustics* (Ed. M. Weydert) publ Elsevier Applied Science (1992) 153-156
15. **Phelps, A.D. and Leighton, T.G.** Investigations into the use of two frequency excitation to accurately determine bubble sizes *Proceedings of IATUM Conference on Bubble Dynamics and Interface Phenomena, Birmingham, UK,* (1993)